

1     **Experimental Study of Overheating of an Unglazed Transpired Collector Façade under Southern**  
2                     **European Summer Conditions for Four Modes of Operation**

3     F. Peci\* [fernando.peci@uco.es](mailto:fernando.peci@uco.es)

4     F. Táboas [francisco.taboas@uco.es](mailto:francisco.taboas@uco.es)

5     M. Ruiz de Adana [manuel.ruiz@uco.es](mailto:manuel.ruiz@uco.es)

6     F. Comino [francisco.comino@uco.es](mailto:francisco.comino@uco.es)

7     Departamento de Química-Física y Termodinámica Aplicada, Escuela Politécnica Superior, 7  
8     Universidad de Córdoba, Campus de Rabanales, Antigua Carretera Nacional IV, km 396, 14072 8

9  
10  
11    **Abstract:**

12    The use of unglazed transpired collector (UTC) façades for air preheating in buildings has been  
13    proved to be an energy saving solution for refurbishing old buildings. However, not all climates are  
14    appropriate for the installation of this type of façade, and in some cases their benefits in winter can  
15    be counterbalanced by the negative effects during summer. There is a risk of overheating and  
16    façade cooling load increase if the system is not operated appropriately in summer. In this study, a  
17    UTC façade cooling load increase was measured in real weather conditions in four different  
18    operating modes. Ambient temperature and solar radiation values were monitored. Surface and air  
19    temperatures were measured in the different layers, and the heat flux through the test cell wall  
20    was registered in two cases, both with and without UTC. The four operation modes combined  
21    mechanical or natural ventilation and air flow direction. Results showed that not ventilating the  
22    façade or using natural ventilation increased the façade cooling load by around 45 %, whereas  
23    outdoor mechanical ventilation produced an increase of 23%. Ventilating with indoor air reduced  
24    heat transfer compared to a non-UTC façade but only when it is integrated into an existing  
25    ventilation system. Cooling load increase due to overheating in the UTC façade was low in all four  
26    modes of operation. UTC façades must be integrated into the building ventilation system to avoid a  
27    cooling load increase during summer, or they must be ventilated with outdoor air if there is no  
28    ventilation system to reduce the impact of overheating.

29  
30    **Keywords:** Unglazed Transpired Collector, Ventilated façade, air preheating, ventilation.

31

33 Over the last few years, more and more renewable energy sources have been incorporated to  
34 construction to reduce the energy consumption from other polluting energy sources. In many  
35 cases, solar energy is the most available source and it can be absorbed and used in many ways:  
36 thermal solar collectors, photovoltaic panels, green roofs, green façades, or simply through glazed  
37 façades. The surface area available in roofs may not be sufficient to take advantage of the solar  
38 irradiance on the building. Thus, it is necessary to also use the building façades.

39 However, some of the currently proposed solutions to incorporate solar collectors or other  
40 elements to building façades present important drawbacks when the objective is to refurbish an  
41 existing building or implement an economically viable system. These problems have been  
42 mentioned by various authors (Zhou & Chen 2010; Kalyanova 2008). In the case of opaque  
43 ventilated façades, their cost is low, and their installation does not require a profound intervention  
44 on the building. An opaque ventilated façade is essentially a solar collector where the absorber is  
45 an opaque steel or aluminium plate, and ambient air is introduced in some way inside the façade,  
46 preheating the air as it flows through the layers into the building. The main disadvantage of this  
47 system is that the collector is directly exposed to ambient air on its outer surface and so it has a  
48 high convection heat loss. An unglazed transpired collector, UTC, system was proposed and  
49 patented to mitigate this negative effect (Hollick 1994).

50 A UTC façade is basically an opaque perforated solar collector. A schematic of a UTC is shown in  
51 figure 1. Solar irradiance is absorbed by the outer layer of the collector, which is made of steel or  
52 aluminium and whose surface is painted in a dark colour to achieve a high solar absorptance. In  
53 order to minimize the heat loss by convection to the exterior, the collector is perforated, and a low-  
54 pressure space is created in its plenum using a fan located downstream. In this way, the external  
55 heat boundary layer is sucked through the pores. Therefore, heat loss is reduced almost to long  
56 wave radiation interchange with the surroundings, which can also be decreased by using a low  
57 emissivity coating (Bokor et al. 2017).

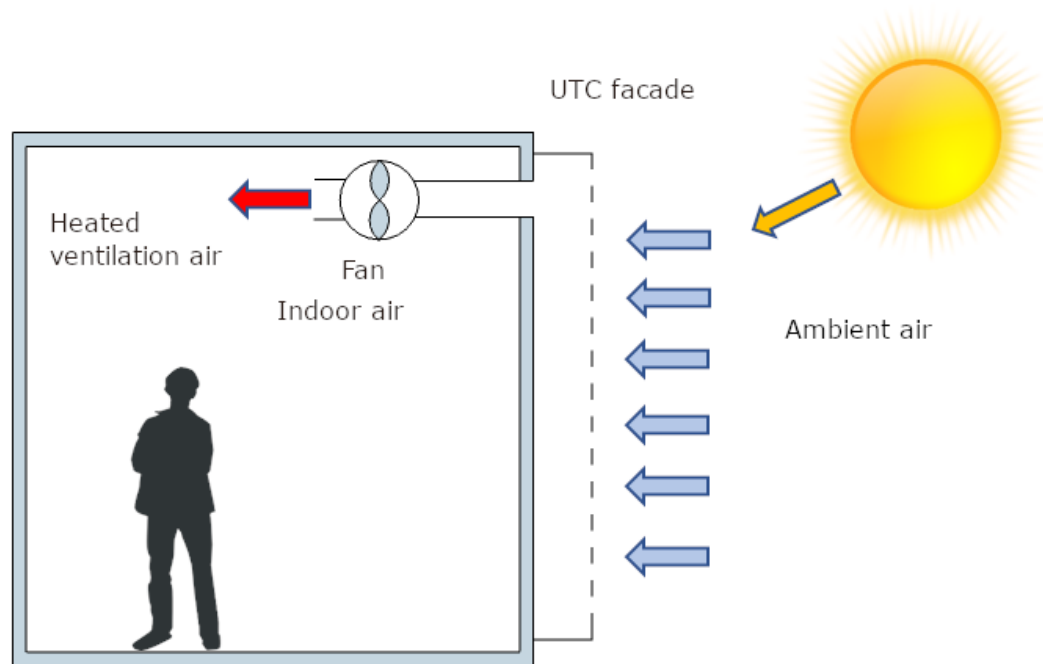
58 UTCs have been widely studied by many authors in the available literature. UTC heat loss due to  
59 natural convection to the ambient air was analysed and found to be negligible, (Kutscher et al.  
60 1993). One of the most influential variables on the performance of a UTC was found to be wind  
61 velocity and many authors have studied its effect on the efficiency of the UTC as a solar collector  
62 (Al-damook & Khalil 2017; Fleck et al. 2002; Vasan & Stathopoulos 2014). UTC façades installed in  
63 residential buildings have also been studied, for instance by (Hollick 1996; Brown et al. 2014).

64 The performance of UTC collectors depends on the climate. In (Peci et al. 2018), the best location to  
65 install UTC façades was found to be in regions with mild winter climates, with many hours of  
66 sunlight and quite high daytime peak temperatures. However, some of these locations also have  
67 dry and hot summer climatic conditions. In these cases, the behaviour of a UTC façade could be  
68 counterproductive during summer because the heated air must be evacuated to avoid overheating  
69 and to avoid an increase in the façade cooling load. Therefore, an appropriate operation mode  
70 should be implemented.

71 Although buildings can benefit from the installation of solar façades in winter, the main problem  
72 arises when the solar collector is working during summer. The air inside the collector can reach high  
73 temperatures (Yu et al. 2017), increasing the heat flow through the insulation wall. Ventilation of  
74 heated air is not required and if not ventilated the air inside the collector increases its temperature  
75 to the point of overheating, and if the existing insulation is poor, the cooling requirements  
76 increase (Stazi et al. 2012). Some authors have studied this effect for other solar walls, such as

77 Trombe walls. However, there are no empirical data in literature regarding the quantification of  
 78 overheating in hot climates during summer for UTC façades. If this is not dealt with adequately, it  
 79 represents an important drawback for its use in building refurbishment. Solutions have been  
 80 proposed by some authors. For example, an increase in the façade insulation was recommended by  
 81 (Long et al. 2018), while ventilation of the collector cavity was the solution proposed by (Stazi et al.  
 82 2012). Another solution is to take advantage of the heat absorbed and use it to heat water or in a  
 83 heat driven cooling system, such as in an absorption cycle or in a desiccant cooling system (Peci et  
 84 al. 2018). In (Soussi et al. 2013), simulations were performed to assess several techniques to  
 85 prevent overheating during summer. However, these solutions lead to increased costs and the  
 86 benefits of preheating air during winter may be exceeded by the initial installation cost.

87 In the present study, an experimental UTC module was built and installed on the façade of a test  
 88 cell under summer weather conditions in Cordoba, Spain. In this location, maximum ambient  
 89 temperatures of around 40 °C are typical. The aim was to quantify the cooling load increase due to  
 90 the UTC façade overheating, comparing with a non-UTC façade. The effects of using four different  
 91 modes of operation to avoid overheating were also evaluated in terms of cooling load decrease.



92

93

Figure 1. Schematic of UTC façade system

94

95 Nomenclature:

96  $E_{daily}$  daily façade cooling load per unit collector area (J)

97  $E_{daily,UTC}$  daily UTC façade cooling load per unit collector area (J)

98  $E_{daily,Non-UTC}$  daily non-UTC façade cooling load per unit collector area (J)

99  $\dot{q}_i$  Heat transfer through the façade ( $W/m^2$ )

100 t time (s)

101

102

## 103 2. Experimental setup

104 An experimental UTC module was manufactured, installed on the south wall of a test cell under real  
105 weather conditions and monitored. This orientation was chosen because the high number of hours  
106 of solar irradiance. Nevertheless, the performance of UTC façades for other orientations was  
107 studied by (Peci et al. 2018). The location of the test cell was Cordoba, in the south of Spain,  
108 coordinates 37°54'51.19''N 4°43'34.8''W. The climate in this location is representative of a  
109 southern European continental climate, with mild winters and very hot and dry summers (Beck et  
110 al. 2018).

111

112 The test cell consisted of a modular site office of 6x2x2.5 m insulated with 3 cm sandwich panels,  
113 see figure 2. The cell had a door and a small window, both closed during the experiments. An air  
114 conditioning system was installed to maintain the indoor temperature within the range of normal  
115 conditions inside a real room. The indoor air temperature was set to 23 °C.

116

117

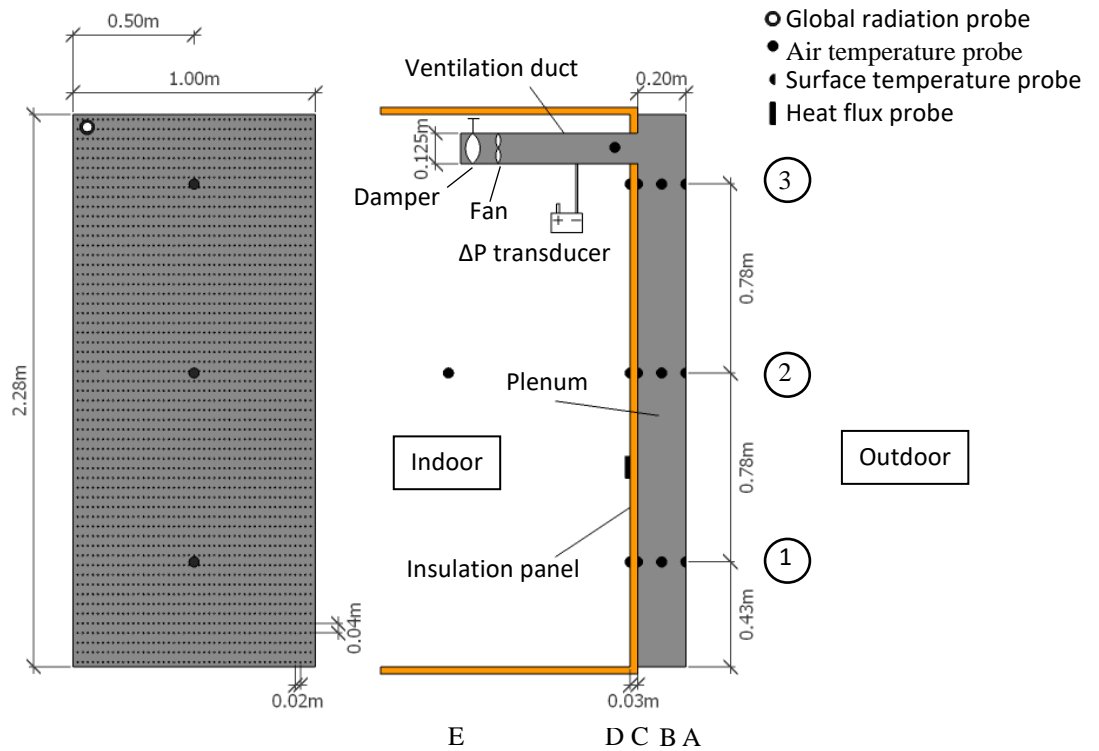


118

119

120 *Figure 2. The test cell. The position of the UTC façade module, the surface temperature probes and the protected ambient*  
121 *temperature probe (right) can be seen.*

122



123

124 *Figure 3. UTC experimental module dimensions and temperature probe locations. Probes were installed at three heights*  
 125 *(1,2 and 3) in the steel plate (A), the plenum (B), the outer sandwich panel surface(C) and the inner sandwich panel surface*  
 126 *(D).*

127 The dimensions of the UTC module are shown in figure 3. The galvanized steel thermal conductivity  
 128 was approximately  $60 \text{ W m}^{-1}\text{K}^{-1}$ , its specific heat  $470 \text{ J kg}^{-1}\text{K}^{-1}$ , and its density  $7800 \text{ kg m}^{-3}$  The test  
 129 cell insulation consisted of a  $0.03 \text{ m}$ -thick sandwich panel with a  $U$ -value of  $0.901 \text{ Wm}^{-2}\text{K}^{-1}$  and a  
 130 weight of  $13.1 \text{ kg m}^{-2}$ . The module was tightened with nuts and bolts to the sandwich panel of the  
 131 south façade of the test cell, and its perimeter sealed with silicone to prevent air leakage. A circular  
 132 hole was made in the upper part of the sandwich panel behind the UTC module which connected  
 133 with the ventilation fan through a  $125 \text{ mm}$  diameter duct. The fan discharged inside the test cell  
 134 through an open damper.

135

136 The configuration of the collector plate was chosen based on the data found in literature. Several  
 137 arrangements of plates and perforations can be found in literature (Van Decker et al. 2001; Li et al.  
 138 2013; Badache et al. 2012). The basic arrangement consists of a metal plate, galvanized steel or  
 139 aluminium, and an array of circular perforations, covering between  $0.8 \%$  and  $5 \%$  of the collector  
 140 surface (Love et al. 2014; Badache et al. 2013). The thickness of plenums varies between  $50$  and  
 141  $300 \text{ mm}$  (Badache et al. 2013; Chan et al. 2014), and the insulation layer can be either an additional  
 142 insulation panel or the existent façade of the building. The latter is frequently the case when  
 143 refurbishing an existent building. An outlet ventilation opening in the upper part of the insulation  
 144 panel connects the plenum with the ducts and the fan that introduces the air stream into the  
 145 indoor space. The normal operation is winter mode, when hot air is introduced directly into the  
 146 building or as preheated air through an existing HVAC system.

147

148

149

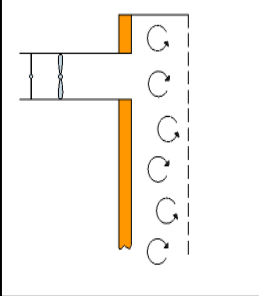
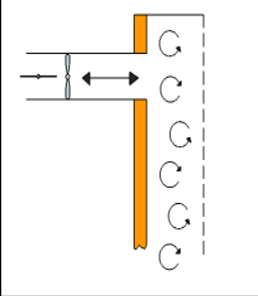
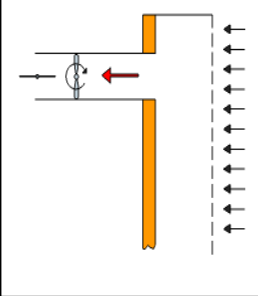
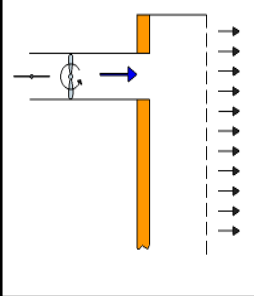
150  
151  
152  
153  
154  
155  
156  
157  
158  
159  
160  
161  
162  
163  
164  
165  
166  
167  
168  
169  
170  
171  
172  
173  
174  
175  
176  
177  
178

Air and surface temperatures were measured using DS18B20 temperature probes, with a maximum error of  $\pm 0.5$  °C. Both the façade with UTC and without UTC were monitored in the same way simultaneously to evaluate the effect of adding a UTC to the test cell façade. The positions of the temperature probes can be seen in figure 2. Two heat flux plates Hukseflux HFP01, (Hukseflux Thermal Sensors n.d.), were installed in the centre of both façades on the inner side of the insulation panel, figure 3.

The weather variables were measured in situ. The ambient temperature was measured just in front of the test cell, see figure 3, and the probe itself was protected against solar radiation. The global solar radiation on the façade surface was measured with a global radiation pyranometer located on the upper right corner of the collector as can be seen in figure 3.

Four operation modes were tested depending on the type of ventilation of the UTC module, see table 1. Modes 1 and 2 corresponded to two situations, one in which the UTC façade is not ventilated, and the other naturally ventilated. This could happen in real-life situations due to a UTC fan failure or a misuse of the system. In modes 3 and 4, the UTC was ventilated, from outdoor to outdoor in the former case and from indoor to outdoor in the latter. In both cases overheating of the façade is prevented. In mode 3 the air was exhausted back to outdoor after removing heat from the collector surface. In mode 4 the intake air entered the space through cracks in the test cell: door, window, joints, etc.

The airflow rate in modes 3 and 4 was estimated from the air velocity measured with a hot wire anemometer in the centre of the duct. Although there were small fluctuations, the flow rate was considered constant with an average value of  $220 \text{ m}^3 \text{ h}^{-1}$  for both directions. The average electric fan power consumption during modes 3 and 4 was 34 W.

| Mode 1                                                                            | Mode 2                                                                            | Mode 3                                                                             | Mode 4                                                                              |
|-----------------------------------------------------------------------------------|-----------------------------------------------------------------------------------|------------------------------------------------------------------------------------|-------------------------------------------------------------------------------------|
| Fan: off<br>Damper: closed<br>Flow: natural                                       | Fan: off<br>Damper: open<br>Flow: natural                                         | Fan: on<br>Damper: open<br>Inlet flow                                              | Fan: on<br>Damper: open<br>Outlet flow                                              |
|  |  |  |  |

180

181 Tests were carried out over a period of four weeks of measurements between 13 June and 12 July,  
 182 one week for each of the operation modes tested. Samples were taken every 10 s and their values  
 183 were averaged and stored every 60 s. The results were smoothed with a one hour moving average  
 184 algorithm.

185 The daily cooling load per unit area due to the heat transfer through both façades was evaluated  
 186 using equation 1, where the heat transfer values  $\dot{q}_i$  were measured with one heat flux probe in each  
 187 case, located in the centre of the façade areas. Since only one probe was used for each façade, the  
 188 results were significant only for comparison studies. The cooling load increase percentage when  
 189 using the UTC façade was calculated with equation 2.

190

$$191 \quad E_{daily} = \sum_{i=1}^{i=1440} \dot{q}_i \cdot t \quad (1)$$

192

$$193 \quad \Delta E_{daily} = \frac{E_{daily,UTC} - E_{daily,Non-UTC}}{E_{daily,Non-UTC}} \cdot 100 \quad (2)$$

194 Where  $E_{daily}$  is the integration of the experimental heat transfer through the insulation panel and  $t$  is  
 195 the sample time step. Since quick temperature variations did not occur, transient phenomena can  
 196 be neglected and equation (1) could be considered a good approximation.

197

198

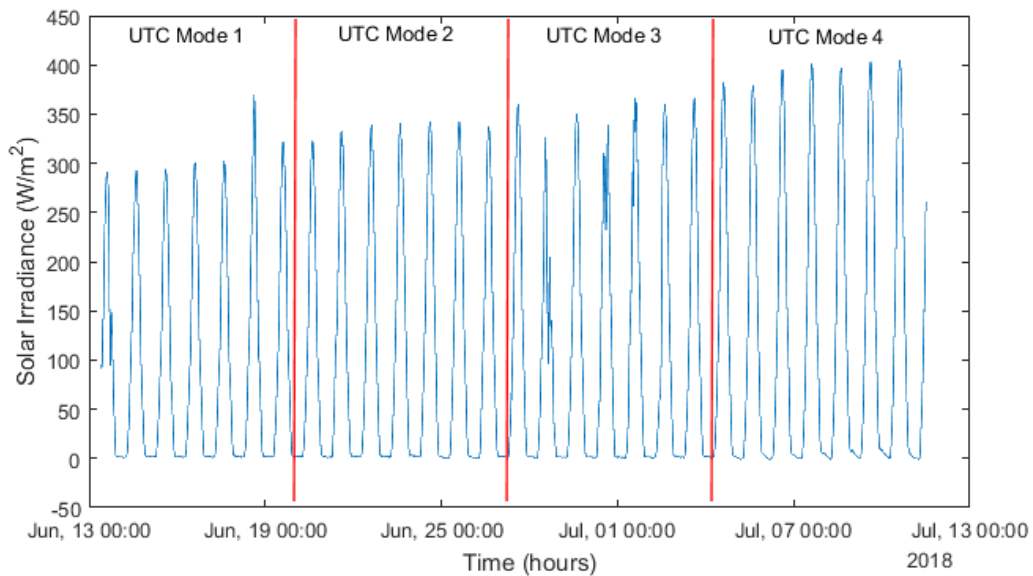
199

### 200 3. Results and analysis

201 The values of the main weather variables, global irradiance on the façade and ambient air  
 202 temperature, during the tests can be seen in figures 4 and 5, respectively. They correspond to  
 203 typical summer weather in the continental dry climate of the south of Spain. The global irradiance  
 204 on the UTC surface showed that the measurements were taken, in general, during hot sunny days,  
 205 figure 4. The peak values during the 28 days of measurements were quite uniform, around 350  
 206  $W/m^2$ . The effect of the peak irradiance will be discussed later.

207 In figure 5, the indoor temperatures and the ambient temperatures just outside the UTC module  
208 registered during the tests are shown. These temperature values are typical for this location at this  
209 time of the year. The ambient air temperature measured corresponded to the temperature of the  
210 air entering the UTC module in mode 3. The peak values were quite uniform, around 40 °C, during  
211 all the tests except for the third week, which was more cloudy and peak temperature values  
212 dropped to around 35 °C. The effect of ambient peak temperatures on the increase of heat transfer  
213 through the façade will be dealt with later. The indoor temperatures oscillated around 24°C during  
214 the day when the air conditioning system was operating. However, during the night there was no  
215 heating system, so the temperature fell naturally to values between 15 °C and 20 °C.

216 From the weather data, it can be concluded that the testing period is appropriate to obtain data of  
217 the UTC performance under unfavourable conditions.

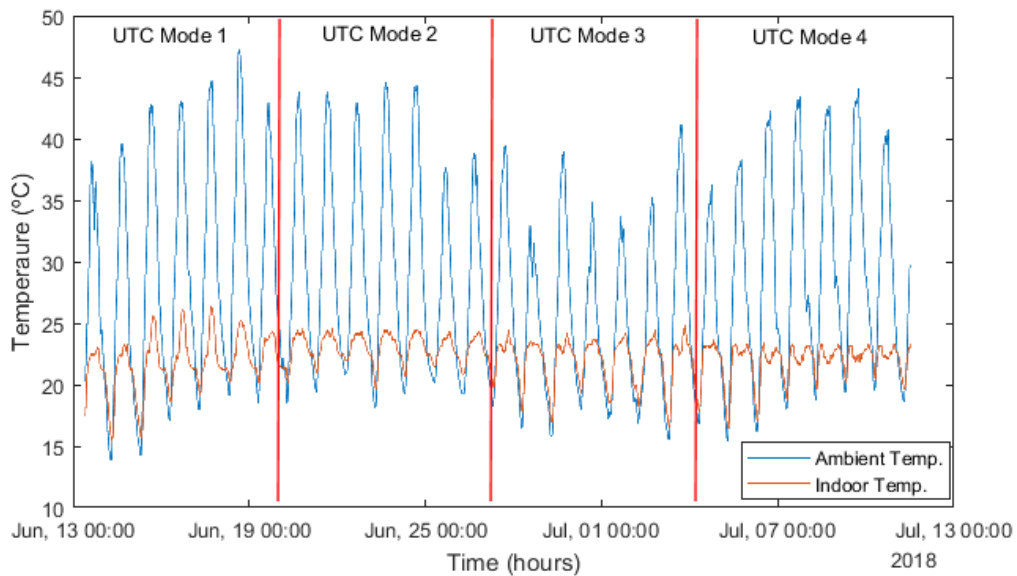


218

219

Figure 4. Solar irradiance on the UTC during the tests

220



221



222

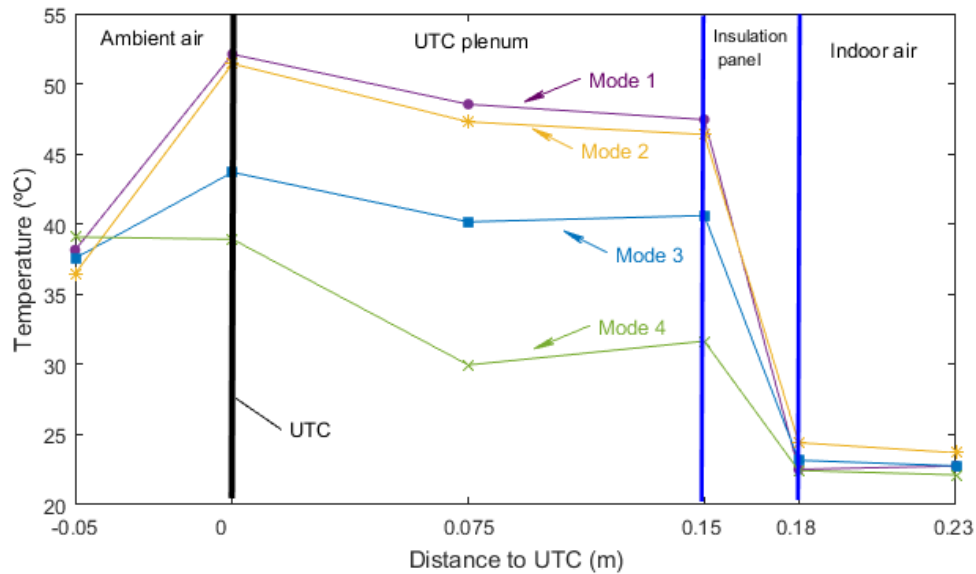
*Figure 5. Ambient and indoor temperatures during the tests*

223

#### 224 **UTC temperature profiles**

225 The temperature profiles across the UTC façade for the maximum and minimum ambient  
226 temperatures are shown in figures 6 and 7. These temperatures were averaged for heights 1, 2 and  
227 3, see figure 3. Similar values of indoor and ambient temperatures and solar radiation were  
228 selected for comparison purposes. Modes 1 and 2 showed similar temperature gradients inside the  
229 plenum and in the insulation layer, thus leading to similar values of heat flux, as figure 6 also shows.  
230 Therefore, the heat transfer from the air in the plenum was not influenced by the opening of the  
231 damper. The reason for this is the small duct diameter compared to the cross section of the UTC  
232 plenum. Natural convection of air through the duct was negligible. The result was that the air in the  
233 plenum was overheated and that caused the heat flux to increase over that of the non-UTC façade,  
234 especially when solar radiation and ambient temperature were at their peak values. Modes 3 and 4  
235 presented more moderate UTC temperatures, as heat was being removed from it due to the  
236 circulation of air through the UTC holes. Therefore, the air temperature inside the plenum did not  
237 reach such high temperatures as in modes 1 and 2. In the case of mode 4 the inverse flow of air  
238 through the façade caused the UTC plate temperature to match approximately the ambient air  
239 temperature. In this case, the plenum air coming from indoors absorbs heat from the UTC and is  
240 then exhausted. Very low air temperatures were obtained in the plenum and the heat flux values  
241 were the lowest. It should be noted that in order to balance the airflow in the test cell, hot air from  
242 the ambient air is introduced through windows and door cracks, thus increasing the cooling load of  
243 the room. This case is only considered if the room ventilation rate is higher than the UTC ventilation  
244 rate, otherwise the increase in cooling load would have to be accounted for in the general balance.

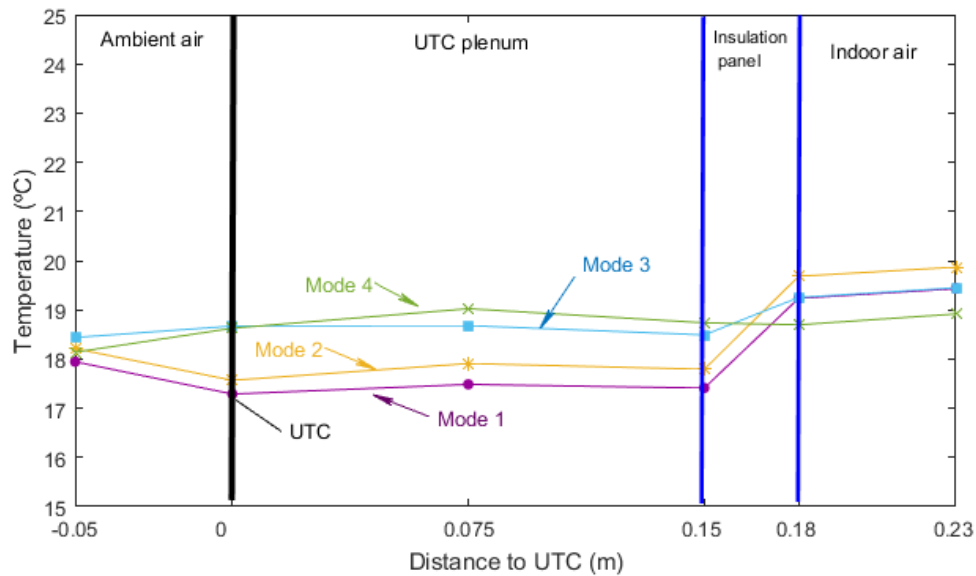
245 Regarding temperature profiles during the night, figure 7, operation modes 1 and 2 presented  
246 similar behaviour with the UTC acting as a radiation shield. In these modes plenum temperatures  
247 were lower than in modes 3 and 4, in which the temperature profiles were flatter. The temperature  
248 differences between modes were not significant but modes 3 and 4 had the advantage of being  
249 able to remove cooling loads during the night through ventilation with fresh air, also known as free  
250 cooling.



251

252 *Figure 6. Temperature profile across the UTC and insulation panel at maximum day temperature in the four modes tested*

253



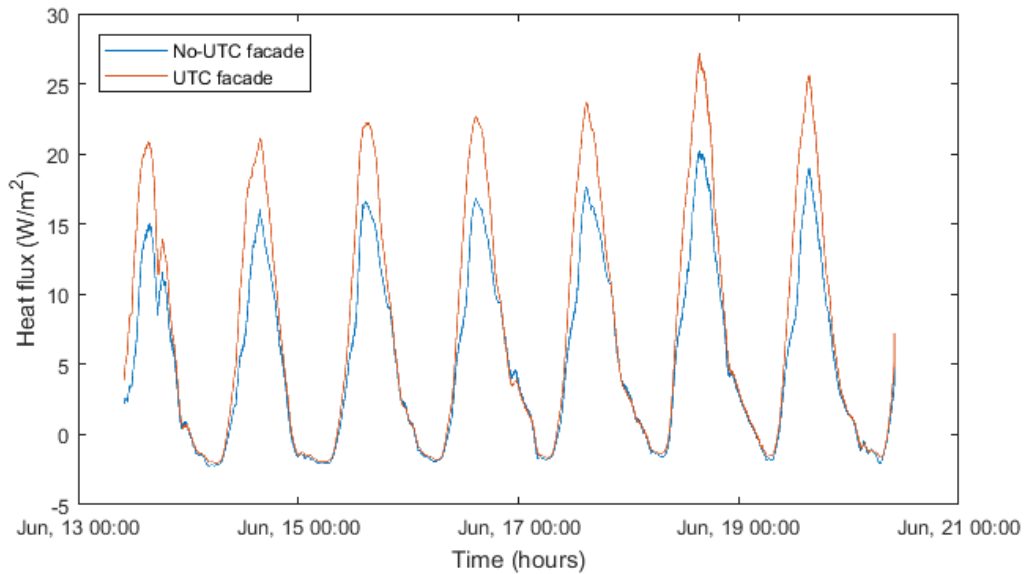
254

255 *Figure 7. Temperature profile across the UTC and insulation panel at minimum day temperature in the four modes tested*

256 **Heat flux increase**

257 a. Mode 1

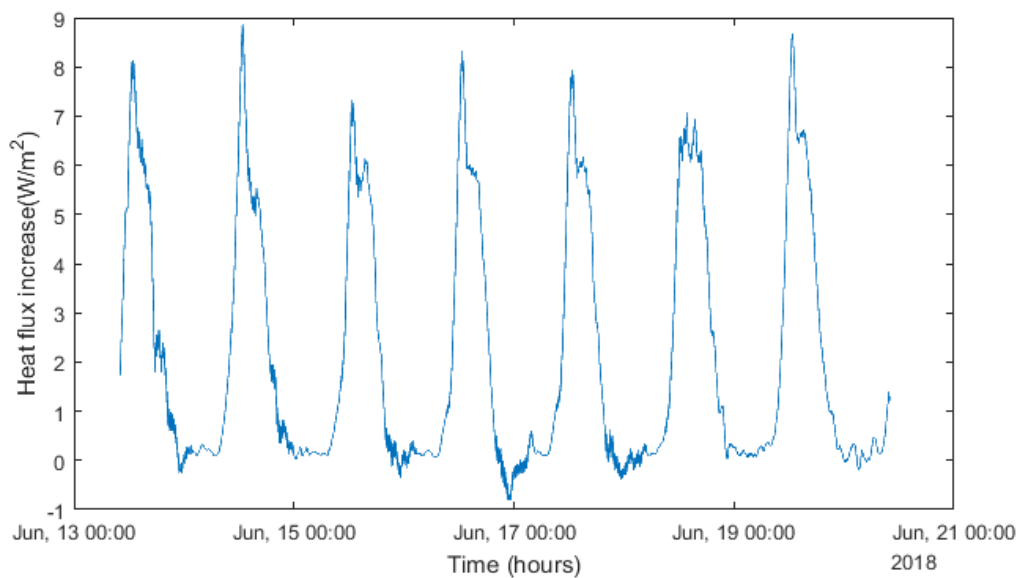
258 Figure 8 shows the heat flux into the test cell through the UTC façade and the non-UTC façade.  
 259 Since the façade was closed and there was no mechanical ventilation, the air in the plenum was  
 260 heated by the UTC plate and temperatures reached high values during peak solar radiation values.  
 261 For this reason, heat flux values for the UTC façade were up to 8 W/m<sup>2</sup> higher than in the case  
 262 without UTC, as can be seen in figure 9. In this mode, the only heat transfer mechanism to evacuate  
 263 the heat absorbed by the UTC was natural convection from the outer surface of the collector, as the  
 264 plenum is sealed. During the night, temperature difference between ambient air and plenum air  
 265 was almost negligible, and heat flux values were similar in both cases.



266

267

Figure 8. Heat flux across the module wall for the UTC and non-UTC façades in mode 1



268

269

Figure 9. Heat flux increase when using the UTC façade in mode 1

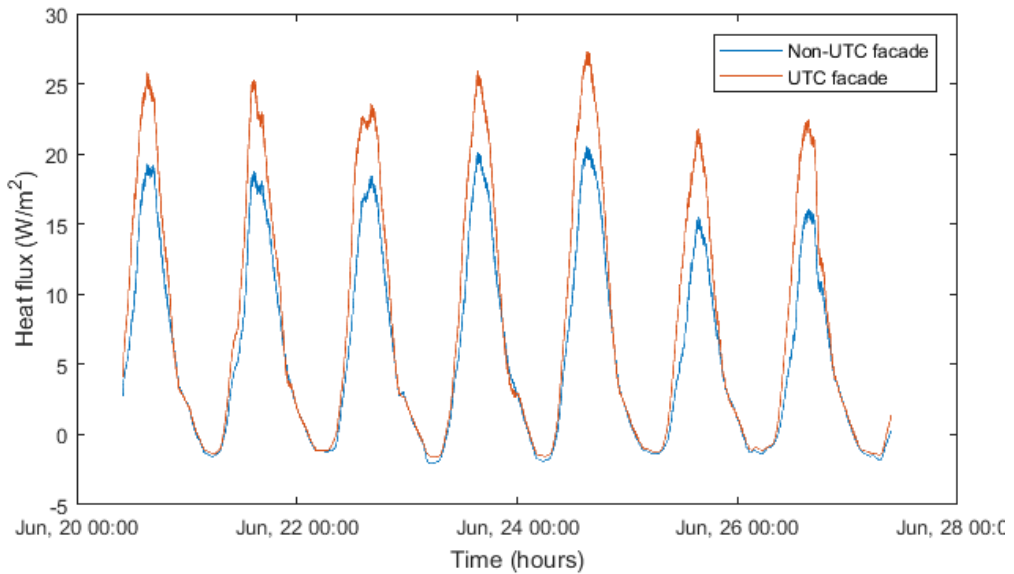
270

b. Mode 2

271

There were no significant differences between this operation mode and mode 1. High temperatures were found inside the UTC and the heat flux values were similar to those in mode 1. Peak and daily values were found to be similar too, figures 10 and 11. In this mode, natural convection evacuates heat from both surfaces of the solar collector layer, and hot air in the plenum is exhausted due to buoyancy, although the results show this effect to be negligible.

276

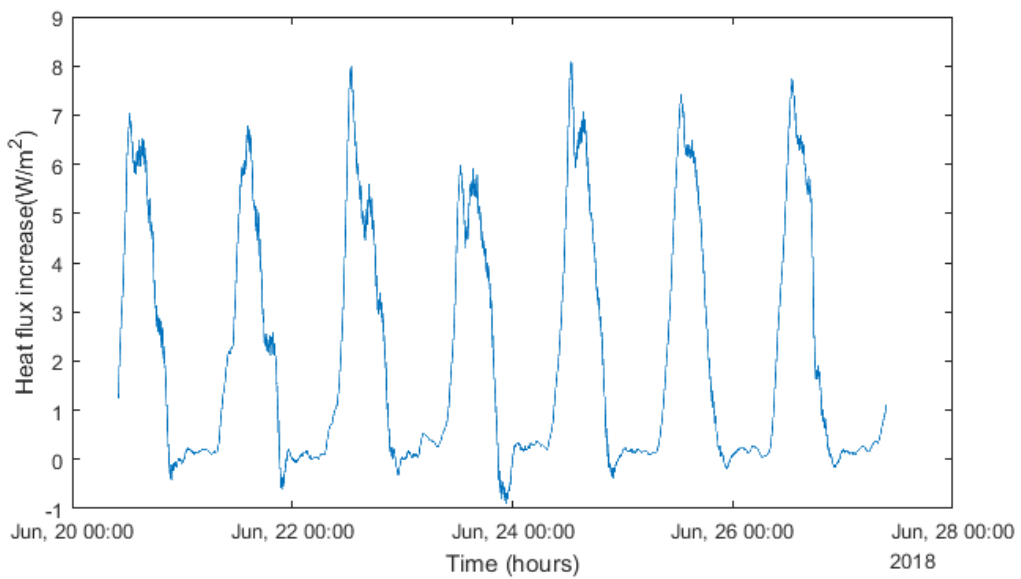


277

278

Figure 10. Heat flux across the module wall for the UTC and non-UTC façades in mode 2

279



280

281

Figure 11. Heat flux increase when using the UTC façade in mode 2

282

283

284

285

c. Mode 3

286

In operation mode 3, figures 12 and 13, the heat flux values presented significantly lower values than in modes 1 and 2. The maximum heat flux peak values were around 2.5 W/m<sup>2</sup> during the day. The daily cooling load increase was between 2.2 % and 13.3 %. In contrast, night values were found to be lower in the case of the UTC façade. Forced convection through the façade increased dramatically the heat removal from the collector layer. The plenum air temperature was still higher than outdoors, but considerably lower than in modes 1 and 2.

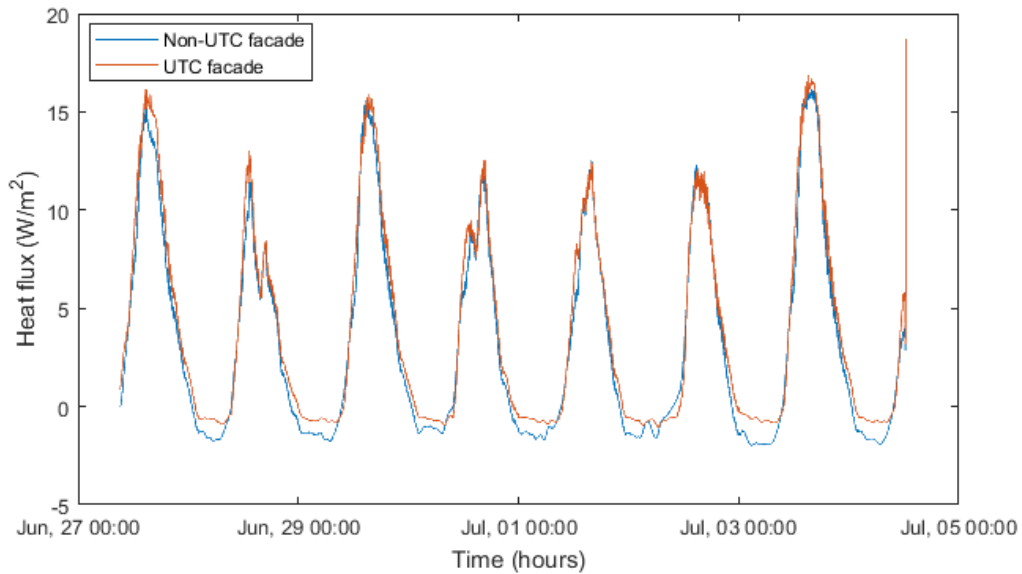
287

288

289

290

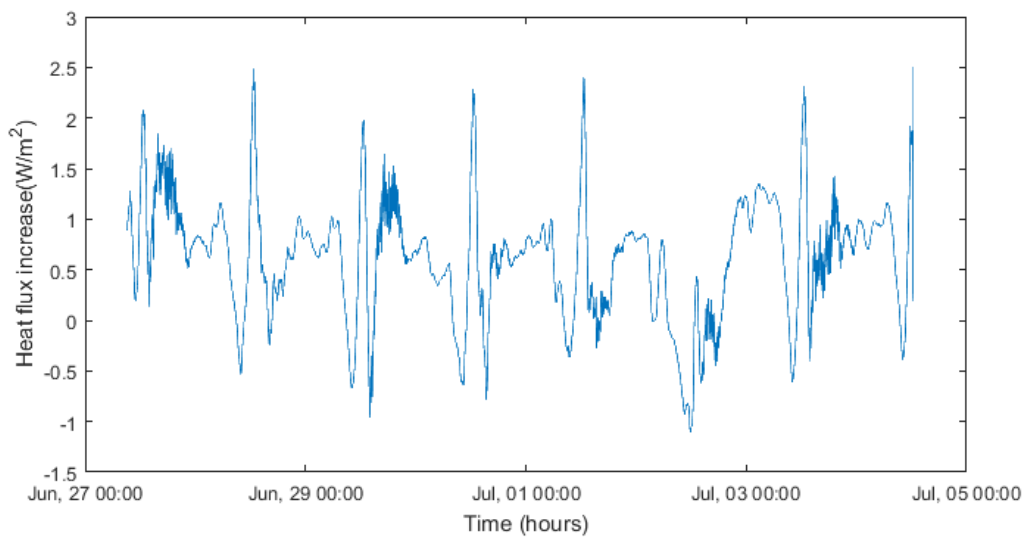
291



292

293

Figure 12. Heat flux across the module wall for the UTC and non-UTC façades in mode 3



294

295

Figure 13. Heat flux increase when using the UTC façade in mode 3

296

297

d. Mode 4

298

299

300

301

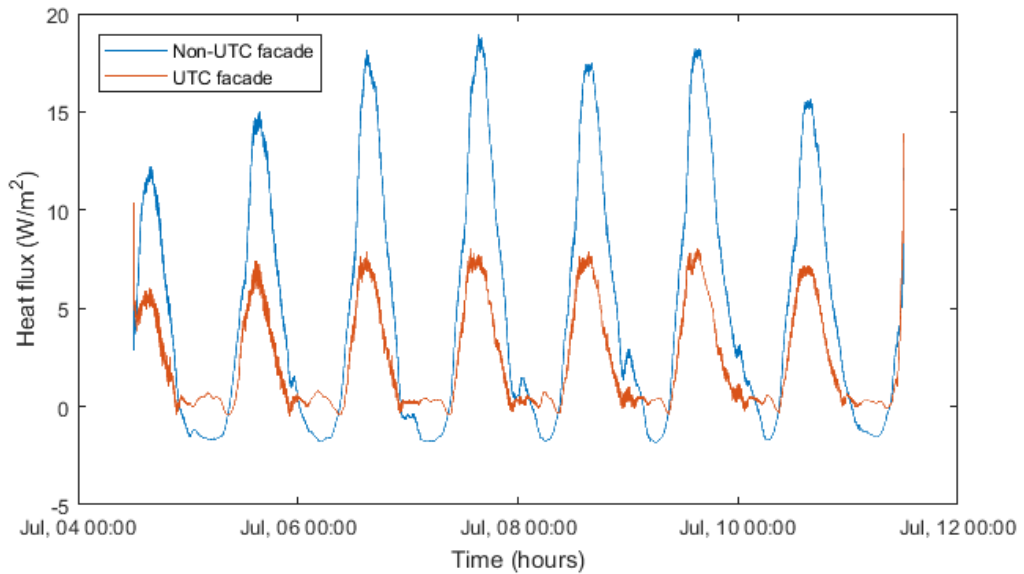
302

303

304

305

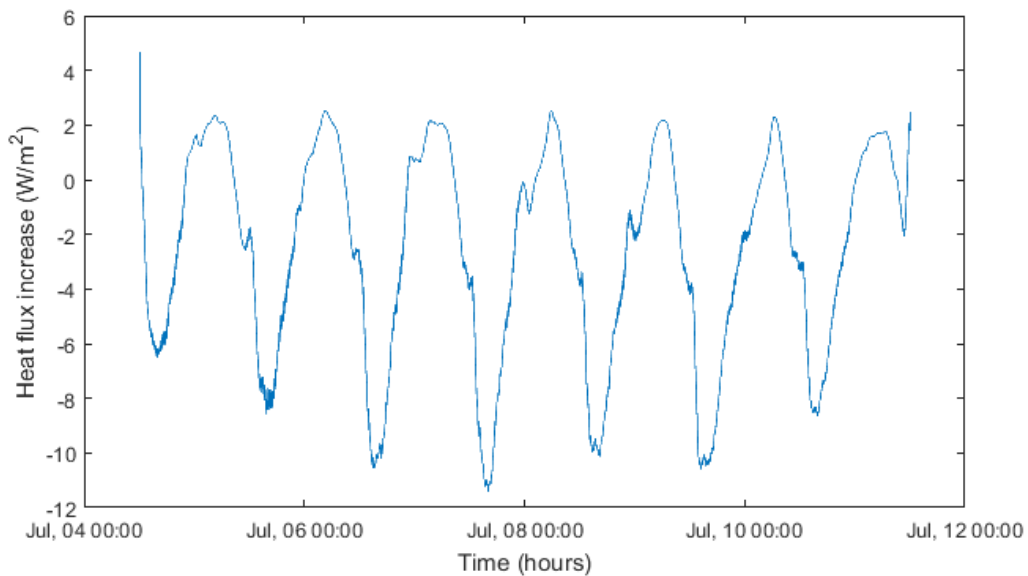
In mode 4, heat flux values were lower in the case of the UTC façade during the day, figure 14. A maximum heat flux decrease of around 11 W/m<sup>2</sup> was measured, figure 15. Daily cooling load values varied between 13.2 kJ/m<sup>2</sup> and 43.2 kJ/m<sup>2</sup>. Heat flux was reduced to almost zero during the night in the case of UTC. Peak values did not follow the same trend as solar irradiance values. In modes 4, convection heat transfer was in this case to indoor air, which was at a lower temperature than outdoors. Moreover, heat was removed after passing through the plenum, so temperatures on either side of the insulation panel were almost the same, leading to very low heat transfer rates through it.



306

307

Figure 14. Heat flux across the module wall for the UTC and non-UTC façades in mode 4



308

309

Figure 15. Heat flux increase when using the UTC façade in mode 4

310

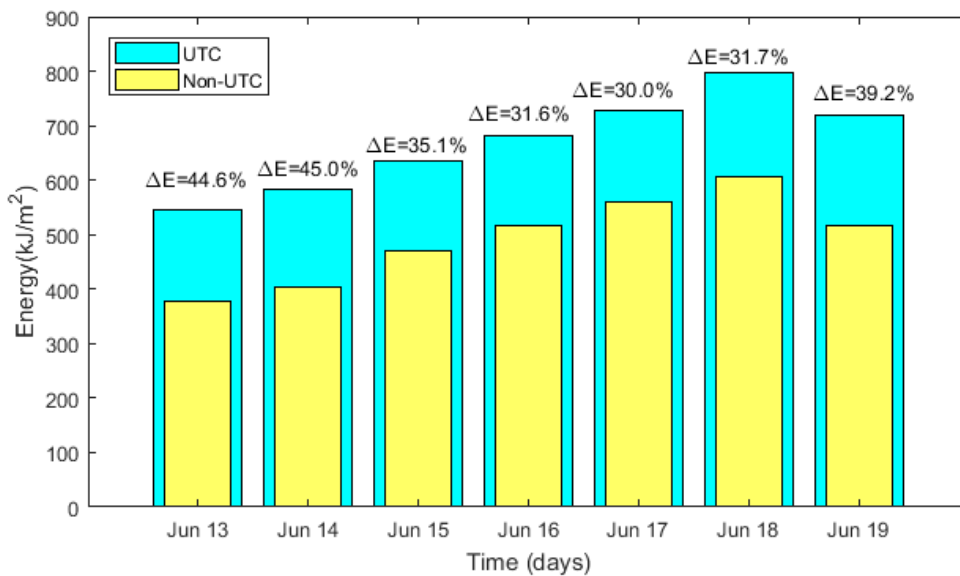
311 In conclusion, modes 1 and 2 would be the inadequate modes of operation for a UTC façade, or  
 312 when mechanical ventilation fails in unfavourable climatic conditions. These operation modes  
 313 should not be used in normal operation during summer. Mode 3 reduces the overheating and does  
 314 not have any drawbacks, providing the hot air from the UTC is exhausted to the exterior. Mode 4 is  
 315 more efficient, and even reduces the cooling load of the façade. The reduced cooling load is only  
 316 possible if there is an existent ventilation system whose exhaust stream is directed through the UTC  
 317 façade. If a ventilation system were not present, a new cooling load would be created and the  
 318 decrease in heat flux through the façade would be balanced with the additional ventilation heat  
 319 gain created.

320

321 **Daily energy gain**

322 Figures 16 to 19 represent the daily integrated energy transferred through the test cell façade,  
323 which was evaluated using equation 2, for all four operation modes, both with and without UTC.  
324 The energy increase, equation 1, is expressed above each bar as a percentage of the energy  
325 transferred through the façade without UTC.

326 Regarding modes 1 and 2, figures 16 and 17, despite the fact that the ambient temperature was  
327 different for each test, the energy increase values were very similar, between 30 % and 45 %. It can  
328 also be noted in these modes that the absolute difference between the daily energy values was not  
329 significantly affected by the meteorological variables. The explanation for this similar behaviour in  
330 these two cases could be the null effect of the aperture of the exhaust damper on the natural  
331 convection air movement inside the UTC plenum, as the duct section area was four times smaller  
332 than the plenum horizontal section. Moreover, the interior room did not have any openings to  
333 create a pressure gradient negative enough for the airflow rate to increase. Nevertheless, the  
334 increase in cooling loads did not reach excessively high absolute values.



335

336

Figure 16. Daily energy gained through the wall for the UTC and non-UTC façades for mode 1

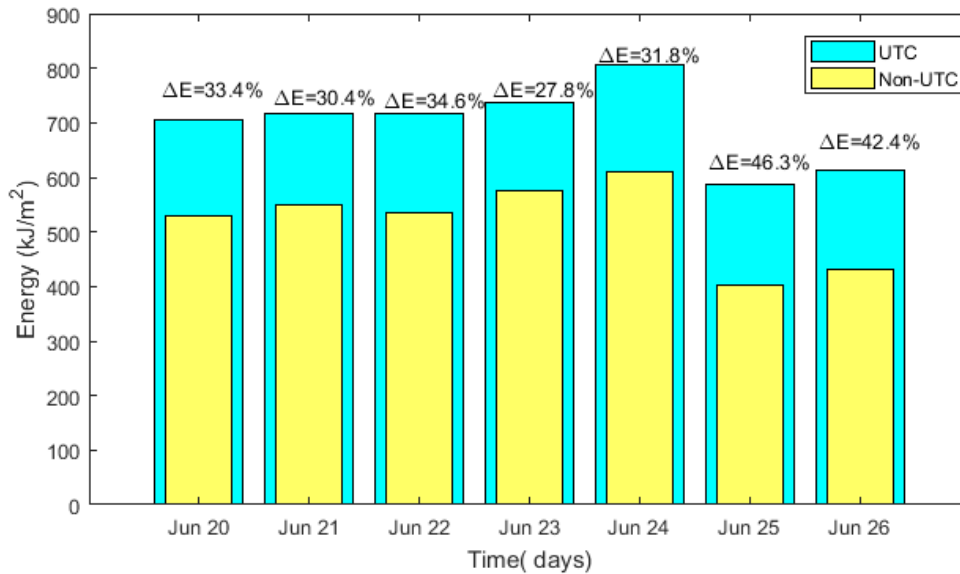


Figure 17. Daily energy gained through the wall for the UTC and non-UTC façades for mode 2

337

338

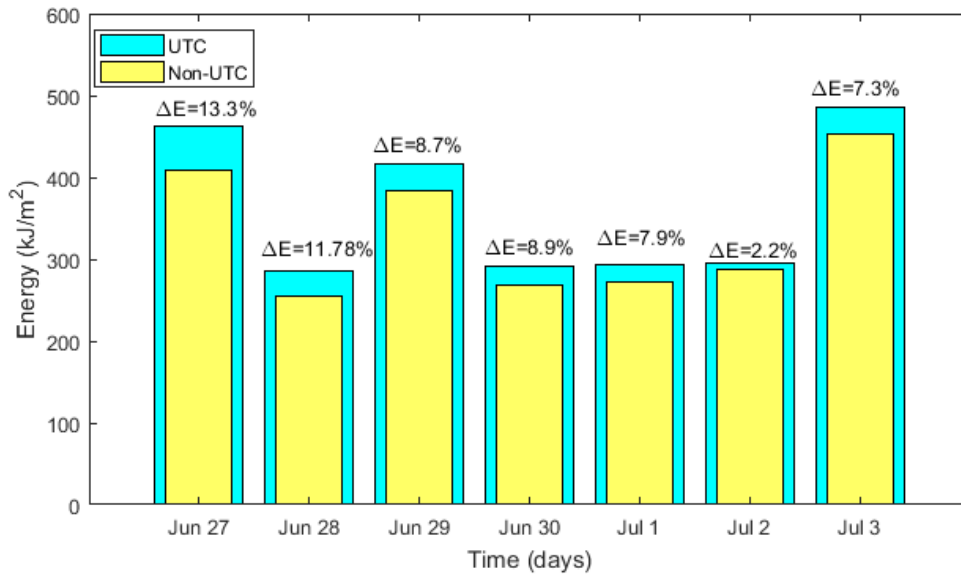
339

340 In contrast, modes 3 and 4, figures 18 and 19, which used mechanical ventilation, showed improved  
 341 behaviour compared to modes 1 and 2, from the façade cooling load point of view. In the case of  
 342 mode 3, figure 18, ventilating the UTC module by suctioning the air through the collector plate and  
 343 then exhausting the air back to the exterior through the duct, produced values of daily energy  
 344 transfer increase between 2.2 % and 13.3 %, lower than in modes 1 and 2. The absolute values  
 345 were correlated to the ambient temperature, as can be seen comparing figure 5 with figure 16.  
 346 However, the energy increase didn't seem to be clearly related either to ambient temperature or to  
 347 solar radiation.

348 In mode 4, figure 19, there was a decrease of energy transfer when using the UTC façade, as the  
 349 UTC ventilation air was indoor air at temperatures around 25 °C, while the ambient temperature  
 350 reached a maximum of around 40 °C. The decrease in energy transfer was clearly correlated with  
 351 the ambient temperature, see figure 5. The ventilation air intakes were cracks in the door, the  
 352 window and other elements of the test cell, so ventilating in this way leads to an increase in  
 353 ventilation cooling load. this option is only justified if an existent ventilation system is present. The  
 354 estimation of the daily cooling load increase due to the infiltration air intake is represented in figure  
 355 20. It shows that the cooling load due to heat transfer through the façade was negligible compared  
 356 to the ventilation cooling load. Therefore, the only case in which ventilation through the façade  
 357 with indoor air would be viable is when there is an existent ventilation system. If there is no  
 358 ventilation system, there would be an unnecessary increase in the building cooling load.

359

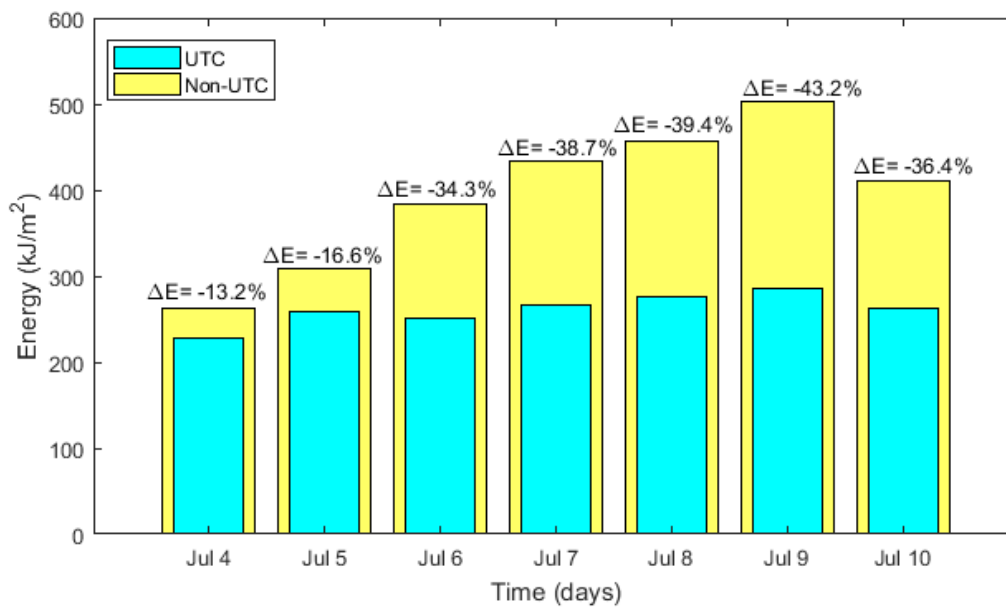




360

361

Figure 18. Daily energy gained through the wall for the UTC and non-UTC façades for mode 3



362

363

Figure 19. Daily energy gained through the wall for the UTC and non-UTC façades for mode 4

364

365

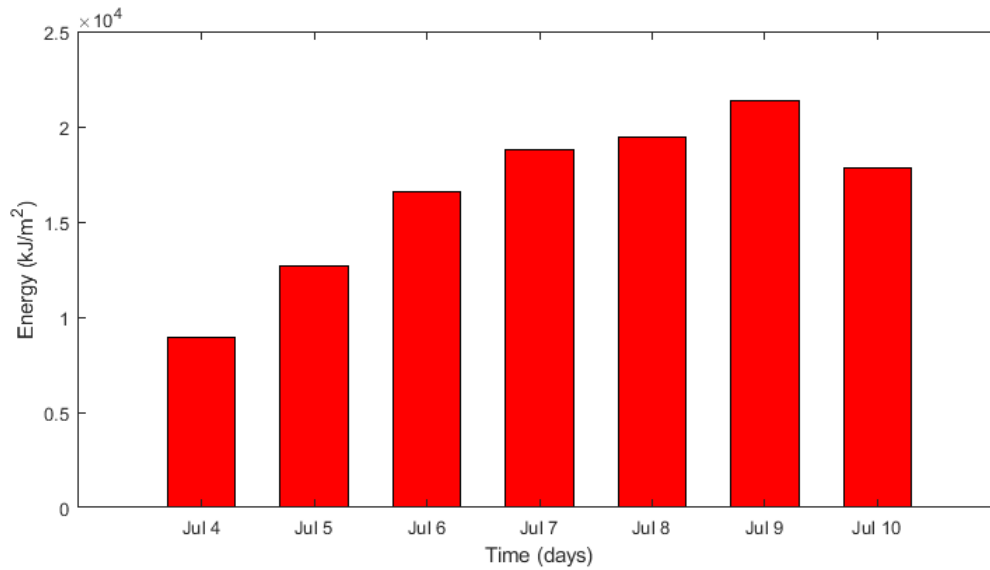


Figure 20. Daily ventilation cooling load increase due to the infiltration air intake in mode 4

366

367

368

369 Table 2 shows the average temperature and global solar radiation for each operation mode  
 370 together with the total cooling load increase due to the UTC façade, the total cooling load in the  
 371 case of non-UTC façade and the percentage of energy increase. Average temperatures and solar  
 372 irradiation were of the same order of magnitude, so comparison between these cases was possible.  
 373 To confirm this point, figure 21 shows the average heat flux through the non-UTC and UTC facades  
 374 within an interval of high solar irradiation and temperature values for the four weeks of  
 375 measurements. It can be seen that in the case of non-UTC façade the heat flux is independent of  
 376 modes of operation, whereas in the case of UTC heat flux follows the same trend that has been  
 377 observed in the previous results. Non-ventilation of the UTC façade increases the cooling load by up  
 378 to 39.4%. Ventilating the façade with ambient air increased the cooling load by 17.2 %, and the fan  
 379 energy consumption is taken into account in the total energy balance. Ventilating with indoor air  
 380 reduced the cooling load, but only in the cases where mechanical ventilation was legally required,  
 381 otherwise the ventilation cooling load is 40 times higher than with the non-UTC façade.

382 The electric power rate of the inline fan was measured, and its mean value was 34 W. In modes 1  
 383 and 2 the fan was off, and this value was irrelevant, but in modes 3 and 4 the energy that the fan  
 384 consumes must be considered. The fan power rate per unit area for the module tested was 14.9 W  
 385 m<sup>-2</sup>, which was of the same order as the maximum heat transfer through the façade at midday, see  
 386 figures 12 and 14. Therefore, preventing overheating through ventilation in mode 3 would not be  
 387 justified, because the decrease in façade cooling load is lower than the total energy consumption of  
 388 the fan. In the case of mode 4, as mentioned above, it is assumed that an existent ventilation  
 389 system was present, so the fan energy consumption would not add any additional energy  
 390 consumption to the system.

391

392

393

394

395  
396

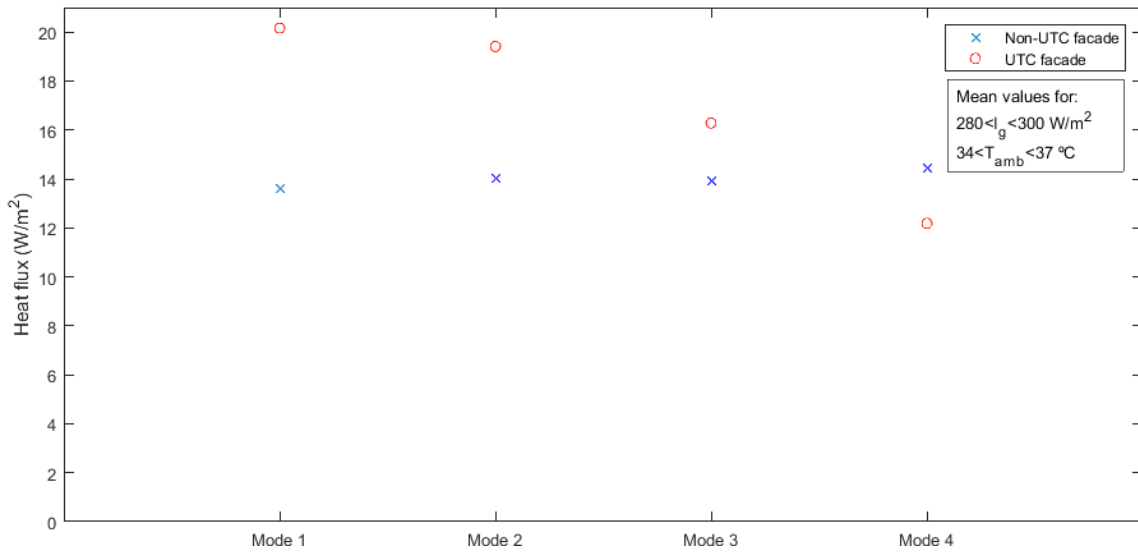
Table 2. Total weekly integrated energy increase for each operation mode and averaged ambient air temperature and solar irradiance during the total test period

| Mode | T <sub>avg</sub> (°C) | I <sub>avg</sub> (W/m <sup>2</sup> ) | ΔE (MJ/m <sup>2</sup> ) | E Non-UTC (MJ/m <sup>2</sup> ) | Δ E (%) | ΔE(%) Including ventilation cooling load | Fan energy consumption (MJ/m <sup>2</sup> ) |
|------|-----------------------|--------------------------------------|-------------------------|--------------------------------|---------|------------------------------------------|---------------------------------------------|
| 1    | 33.1                  | 150                                  | 1.27                    | 3.22                           | 39.4    | 39.4                                     | 0                                           |
| 2    | 33.4                  | 172                                  | 1.27                    | 3.46                           | 36.7    | 36.7                                     | 0                                           |
| 3    | 28.7                  | 170                                  | 0.34                    | 1.98                           | 17.2    | 17.2                                     | 1.4                                         |
| 4    | 32.9                  | 196                                  | -1.58                   | 2.92                           | -54.1   | 4009*                                    | 1.4                                         |

397

\*only in case of non-existing ventilation system

398



399

Figure 21. Average heat flux for high temperature and irradiation values during the four weeks of measurements

400

401

402

#### 4. Conclusions

403

In this study, experimental data were obtained to quantify the influence of a UTC façade on the façade cooling load during hot weather conditions. Four operation modes were tested to quantify the cooling load reduction and to find the most effective. Temperatures and heat transfer through walls, with and without a UTC façade, were measured to obtain comparative results. High ambient temperatures and high values of solar radiation were reached during the tests, which resulted in overheating of the plenum of the UTC façade

409

During the day, it was found that not mechanically ventilating the UTC, modes 1 and 2, increased the plenum air temperature and therefore the heat transfer through the building wall, increasing the cooling load of the building. Natural ventilation was found not to be enough to reduce this effect. At night the effect of the UTC on the different surface temperatures was negligible.

413

Ventilating the UTC façade reduced the cooling load notably during the day. In the case of mode 3, ventilating with ambient air reduced the façade load increase, but required the additional energy consumption of the fan. Ventilating to the exterior, mode 4, was found to reduce the façade cooling load, but as in case 3, the fan energy consumption must be considered in the energy balance.

417

Furthermore, the ventilation cooling load was very high, so this mode can only be considered when a ventilation system already exists in the building.

418

419 Finally, assuming that the building façade is well insulated, the cooling load increase found in this  
420 study due to the installation of a UTC façade may not justify the use of a fan, so mode 3 is not  
421 recommended. Modes 1 and 2 are recommended, as the overheating was found not to be high  
422 enough to cause a high cooling load increase. Mode 4 is only recommended in the case of an  
423 existing ventilation system.

424 For future work, it would be interesting to study the minimum airflow rate needed to nullify the  
425 cooling load increase for a particular insulation wall, as in this paper the nominal air flow rate for  
426 winter was used.

427

## 428 **References**

429

430 Al-damook, A. & Khalil, W.H., 2017. Experimental evaluation of an unglazed solar air collector for  
431 building space heating in Iraq. *Renewable Energy*, 112, pp.498–509. Available at:  
432 <http://www.sciencedirect.com/science/article/pii/S0960148117304378>.

433 Badache, M. et al., 2013. Experimental and numerical simulation of a two-dimensional unglazed  
434 transpired solar air collector. *Solar Energy*, 93, pp.209–219. Available at:  
435 <http://www.sciencedirect.com/science/article/pii/S0038092X1300145X>.

436 Badache, M., Hall??, S. & Rouse, D., 2012. A full 3 4 factorial experimental design for efficiency  
437 optimization of an unglazed transpired solar collector prototype. *Solar Energy*, 86(9),  
438 pp.2802–2810.

439 Beck, H.E. et al., 2018. Present and future Köppen-Geiger climate classification maps at 1-km  
440 resolution. *Scientific Data*, 5, p.180214. Available at: <https://doi.org/10.1038/sdata.2018.214>.

441 Bokor, B. et al., 2017. Theoretical and experimental analysis on the passive cooling effect of  
442 transpired solar collectors. *Energy and Buildings*, 156, pp.109–120. Available at:  
443 <http://www.sciencedirect.com/science/article/pii/S0378778817315153>.

444 Brown, C. et al., 2014. Transpired solar collector installations in Wales and England. *Energy*  
445 *Procedia*, 48, pp.18–27. Available at: <http://dx.doi.org/10.1016/j.egypro.2014.02.004>.

446 Chan, H.Y. et al., 2014. Thermal analysis of flat and transpired solar facades. *Energy Procedia*, 48,  
447 pp.1345–1354. Available at: <http://dx.doi.org/10.1016/j.egypro.2014.02.152>.

448 Van Decker, G.W.E., Hollands, K.G.T. & Brunger, A.P., 2001. Heat-exchange relations for unglazed  
449 transpired solar collectors with circular holes on a square or triangular pitch. *Solar Energy*,  
450 71(1), pp.33–46.

451 Fleck, B.A., Meier, R.M. & Matovic, M.D., 2002. a Field Study of the Wind Effects on the  
452 Performance of an Unglazed Transpired Solar Collector. *Solar Energy*, 73(3), pp.209–216.  
453 Available at: [www.elsevier.com](http://www.elsevier.com).

454 Hollick, J.C., 1996. S LARGEST AND TALLEST SOLAR RECLADDING Solarwall ' Air Heater. , pp.703–  
455 707.

456 Hollick, J.C., 1994. Unglazed solar wall air heaters. *Renewable Energy*, 5(1), pp.415–421. Available  
457 at: <http://www.sciencedirect.com/science/article/pii/0960148194904081>.

458 Hukseflux Thermal Sensors, User Manual HFP01&HFP03 heat flux plate/heat flux sensor. *manual*  
459 v1721. Available at: <https://www.hukseflux.com/uploads/product->

460 documents/HFP01\_HFP03\_manual\_v1721.pdf.

461 Kalyanova, O., 2008. *Double-Skin Facade: Modelling and Experimental Investigations of Thermal*  
462 *Performance*, Available at: <http://forskningbasen.deff.dk/Share.external?sp=Sbd6782e0->  
463 [e607-11dd-b0a4-000ea68e967b&sp=Saau](http://forskningbasen.deff.dk/Share.external?sp=Sbd6782e0-e607-11dd-b0a4-000ea68e967b&sp=Saau).

464 Kutscher, C.F., Christensen, C.B. & Barker, G.M., 1993. Unglazed Transpired Solar Collectors: Heat  
465 Loss Theory. *Journal of Solar Energy Engineering*, 115(3), pp.182–188. Available at:  
466 <http://dx.doi.org/10.1115/1.2930047>.

467 Li, S. et al., 2013. Airflow and thermal analysis of flat and corrugated unglazed transpired solar  
468 collectors. *Solar Energy*, 91, pp.297–315. Available at:  
469 <http://dx.doi.org/10.1016/j.solener.2013.01.028>.

470 Long, J., Yongga, A. & Sun, H., 2018. Thermal insulation performance of a Trombe wall combined  
471 with collector and reflection layer in hot summer and cold winter zone. *Energy and Buildings*,  
472 171, pp.144–154. Available at: <https://doi.org/10.1016/j.enbuild.2018.04.035>.

473 Love, C.D. et al., 2014. Transpired solar collector duct for tempering air in North Carolina turkey  
474 brooder barn and swine nursery. *Solar Energy*, 102, pp.308–317. Available at:  
475 <http://dx.doi.org/10.1016/j.solener.2013.11.028>.

476 Peci, F., Comino, F. & Ruiz de Adana, M., 2018. Performance of an unglazed transpire collector in  
477 the facade of a building for heating and cooling in combination with a desiccant evaporative  
478 cooler. *Renewable Energy*. Available at:  
479 <http://www.sciencedirect.com/science/article/pii/S0960148118300296>.

480 Soussi, M., Balghouthi, M. & Guizani, A., 2013. Energy performance analysis of a solar-cooled  
481 building in Tunisia: Passive strategies impact and improvement techniques. *Energy and*  
482 *Buildings*, 67, pp.374–386. Available at: <http://dx.doi.org/10.1016/j.enbuild.2013.08.033>.

483 Stazi, F., Mastrucci, A. & Di Perna, C., 2012. The behaviour of solar walls in residential buildings with  
484 different insulation levels: An experimental and numerical study. *Energy and Buildings*, 47,  
485 pp.217–229. Available at: <http://dx.doi.org/10.1016/j.enbuild.2011.11.039>.

486 Vasan, N. & Stathopoulos, T., 2014. Experimental study of wind effects on unglazed transpired  
487 collectors. *Solar Energy*, 101, pp.138–149. Available at:  
488 <http://www.sciencedirect.com/science/article/pii/S0038092X13005537>.

489 Yu, G. et al., 2017. Thermal Performance of Building-integrated Solar Wall during Stagnation.  
490 *Procedia Engineering*, 205, pp.183–189. Available at:  
491 <https://doi.org/10.1016/j.proeng.2017.09.951>.

492 Zhou, J. & Chen, Y., 2010. A review on applying ventilated double-skin facade to buildings in hot-  
493 summer and cold-winter zone in China. *Renewable and Sustainable Energy Reviews*, 14(4),  
494 pp.1321–1328. Available at: <http://dx.doi.org/10.1016/j.rser.2009.11.017>.

495